Physiological Measurement

IPEM
Institute of Physics and Engineering in Medicine

In vivo PIV measurement of red blood cell velocity field in microvessels considering mesentery motion

To cite this article: Yasuhiko Sugii *et al* 2002 *Physiol. Meas.* **23** 403

INSTITUTE OF PHYSICS PUBLISHING PHYSIOLOGICAL MEASUREMENT

Physiol. Meas. **23** (2002) 403–416 PII: S0967-3334(02)32600-5

In vivo PIV measurement of red blood cell velocity field in microvessels considering mesentery motion

Yasuhiko Sugii[1], **Shigeru Nishio**[2] **and Koji Okamoto**[3]

[1] Nuclear Engineering Research Laboratory, University of Tokyo 2-22 Shirane, Shirakata, Tokai-mura, Ibaraki, 319-1188, Japan
[2] Department of Maritime Science, Kobe University of Mercantile Marine, 5-1-1, Fukae-Minami, Higashinada, Kobe, 658-0022, Japan
[3] Nuclear Engineering Research Laboratory, University of Tokyo 2-22 Shirane, Shirakata, Tokai-mura, Ibaraki, 319-1188, Japan

E-mail: sugii@tokai.t.u-tokyo.ac.jp

Received 11 January 2002, in final form 22 February 2002
Published 21 March 2002
Online at stacks.iop.org/PM/23/403

Abstract

As endothelial cells are subject to flow shear stress, it is important to determine the detailed velocity distribution in microvessels in the study of mechanical interactions between blood and endothelium. Recently, particle image velocimetry (PIV) has been proposed as a quantitative method of measuring velocity fields instantaneously in experimental fluid mechanics. The authors have developed a highly accurate PIV technique with improved dynamic range, spatial resolution and measurement accuracy.

In this paper, the proposed method was applied to images of the arteriole in the rat mesentery using an intravital microscope and high-speed digital video system. Taking the mesentery motion into account, the PIV technique was improved to measure red blood cell (RBC) velocity. Velocity distributions with spatial resolutions of 0.8×0.8 μm were obtained even near the wall in the centre plane of the arteriole. The arteriole velocity profile was blunt in the centre region of the vessel cross-section and sharp in the near-wall region. Typical flow features for non-Newtonian fluid were shown. Time-averaged velocity profiles in six cross sections with different diameters were compared.

Keywords: blood flow, RBC velocity, microcirculation, highly accurate PIV technique

1. Introduction

Microcirculation in arterioles, capillaries and venules, which have diameters of 5 to 50 μm, is essential in the process of maintaining healthy tissues and organs. In particular, the

measurement of the circulation velocity with high spatial resolution and high measurement accuracy is crucial for scientific and clinical study in evaluating supply to the tissues and organs and the shear stress of blood cells and endothelial cells. Various experimental techniques, such as the electromagnetic blood flowmeter, the ultrasonic Doppler flowmeter, laser Doppler velocimetry, the dual slit method and so on, have been developed to measure blood velocity in microcirculation. The most practical and commonly used method is the dual slit method (Wayland and Johnson 1997, Intaglietta *et al* 1975, Yamaguchi *et al* 1992), which measures the passage of blood flow between two pre-determined points by the dual window method. However, this technique is based on the assumption that blood flow passes both points under the same conditions. In laser Doppler velocimetry (LDV) (Cochrane *et al* 1981, Seki *et al* 1996), a measurement at any probe area is limited to a depth of a few millimeters, which may result in spurious signals and reduce the accuracy of measurement. Since a spatial resolution and measurement accuracy of velocity distribution was not enough to estimate wall shear stress, wall shear stress has been commonly estimated based on a parabolic profile using the flow rate. Several techniques based on microscopic video images have also been proposed, in which a velocity vector was usually obtained by tracking an RBC in two successive images (Tangelder *et al* 1986, 1988, Parthasarahi *et al* 1999, Bishop *et al* 2001). These techniques have limited spatial and temporal resolution depending on the performance of the camera. Tsukada *et al* (2000) applied a conventional image correlation technique, the cross-correlation technique, to *in vivo* blood flow images recorded using a high-speed camera in order to improve resolution. However, the images were not suitable for microcirculation analysis with respect to the measurement accuracy and spatial resolution due to the inadequacies of the image analysis technique.

Particle image velocimetry (PIV) is a quantitative method for measuring velocity fields instantaneously in experimental fluid mechanics systems (Keane and Adrian 1992, Raffel *et al* 1998). A number of PIV methods, such as the cross-correlation method, particle tracking method and iterative correlation method, have been proposed for macro flow to improve measurement accuracy and spatial resolution. The main feature of these methods, measurement accuracy and utility in a range of experimental conditions, has been comprehensively investigated both experimentally and theoretically. Recently, microscopic PIV techniques, using an epi-fluorescent microscope and a CCD camera, have been developed for the measurement of velocity fields in microfluid devices (Santiago *et al* 1998, Meinhart *et al* 1999, Koutsiaris *et al* 1999). Optical effects, particularly the effect of depth of focus, have been investigated (Meinhart *et al* 2000, Olsen and Adrian 2000).

The present authors have developed a highly accurate PIV technique (Sugii *et al* 2000) with improved measurement accuracy and spatial resolution, and have applied it to the analysis of blood flow images in 30 μm diameter bifurcation arteriole using an intravital microscope and high-speed digital video system (Nakano *et al* 2001, Sugii *et al* 2001). It was confirmed that the method was useful for the measurement of blood flow velocity. The results indicated that the dynamics of blood flow were complex due to multi-phase flow, the non-Newtonian fluid, the cardiac cycle and so on. However, the measurement accuracy decreased in different vessels due to a mesentery motion. In order to investigate the dynamics, it is important to improve the measurement accuracy even with a mesentery motion.

In this paper, *in vivo* blood images of a straight arteriole in a rat mesentery were recorded using an intravital microscope and high-speed digital video system. The PIV method was applied to determine mesentery motion, and improved the accuracy of RBC velocity by taking the motion into account. Since blood vessels usually move during blood velocity measurement, the measurement accuracy is low. Axial velocity profiles with high accuracy and high spatial resolution in cross-sections were investigated.

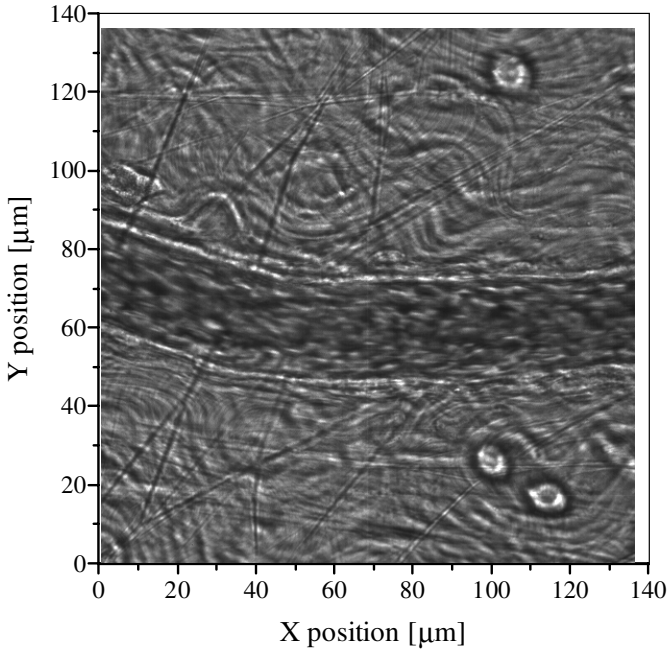

Figure 1. Image of blood flow in arteriole.

2. Experimental set-up and method

2.1. Blood flow image

A mesenteric arteriole of an anesthetized male Wister rat (8 weeks, 310 g body weight) was observed using an intravital microscope with a water immersion objective (CFI Fluor 60 × W, Nikon, Japan), with magnification $M = 60$ and numerical aperture NA $= 1.0$ (see detail in Nakano *et al* 2002). Blood flow images were recorded by a computer for a period of approximately 2 s (2048 images) using a high-speed CCD camera (Weinberger SpeedCAMpro, Dietikon, Switzerland) at 1000 frames s^{-1}. Images were captured at a resolution of 512 × 512 pixels in 8-bit greyscale. The measurement region was backlit using a 250 W direct-current metal halide lamp. The illumination was filtered through a 546 nm green interference filter in order to emphasize the contrast in the RBC images. The basic flow features were initially investigated by examining a relatively straight length of arteriole. Figure 1 shows a captured image of blood flow in a mesenteric arteriole. The observed region was 136 × 136 μm in size, with each pixel representing a 0.27 × 0.27 μm area. The estimated internal diameter of the vessel was 24 to 26 μm. The vessel curved slightly to the right at around $x = 50$ μm. Generally, the diameter of the endothelial cells is approximately 5 μm; however, the apparent diameter of these cells in the present images is 2 to 4 μm. This is considered to be due to the out-of-plane alignment of the cells in the optical plane. A plasma layer in which very few cells passed was clearly observed near the wall.

2.2. Analysis method

The authors previously proposed a highly accurate high-resolution PIV technique (Sugii *et al* 2000). In this PIV method, pixel unit displacement is obtained by using iterative

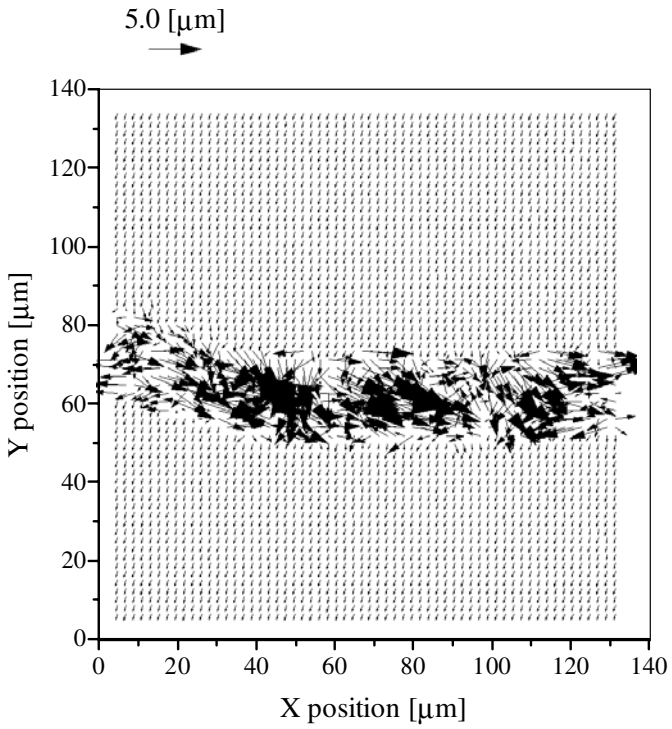

Figure 2. Displacement distribution of mesentery from an initial position, obtained by PIV technique.

cross-correlation, and sub-pixel displacement is calculated by a gradient method. Errors due to the experimental conditions, such as particle diameter, particle density, velocity gradient and out-of-plane velocity, have been analytically assessed through Monte Carlo simulations. From comparisons with generated PIV images with known displacement, the root-mean-square (RMS) error of the measurement technique is of the order of 0.01 pixels, even with the small interrogation window size of 8×8 pixels or less. Thus, the method provides high sub-pixel accuracy and high spatial resolution.

The PIV technique was applied to the first blood image at $t = 0$ as a reference, and then sequentially to subsequent images at $t = k$ ($k = 1, 2 \ldots 2047$). The aim in this analysis was to measure the movement of the mesentery rather than the RBC velocity. The motion of patterns within the mesentery image, such as musculi and vessel walls, was then obtained. The displacement was obtained as the relative distance from the reference image. Figure 2 shows a sample of the displacement distribution of mesentery obtained by this method. The obtained displacement vector showed the movement of each position within the interrogation window from the reference image. The interrogation window was 19×19 with a 50% overlap, corresponding to a spatial resolution of 2.4×2.4 μm. Many spurious vectors were recognized in the inner area of the arteriole around a centre of image. The time interval between analysed images was too long to measure individual RBC displacements, which were greater than the image width between frames. Therefore, some mismatch occurred for the inner area. The displacement vectors in the upper and lower areas of the arteriole, out of vessel area, were used for measuring the movement of the mesentery and the contraction and relaxation of blood vessels. The displacements in the upper and lower areas were approximately -0.52

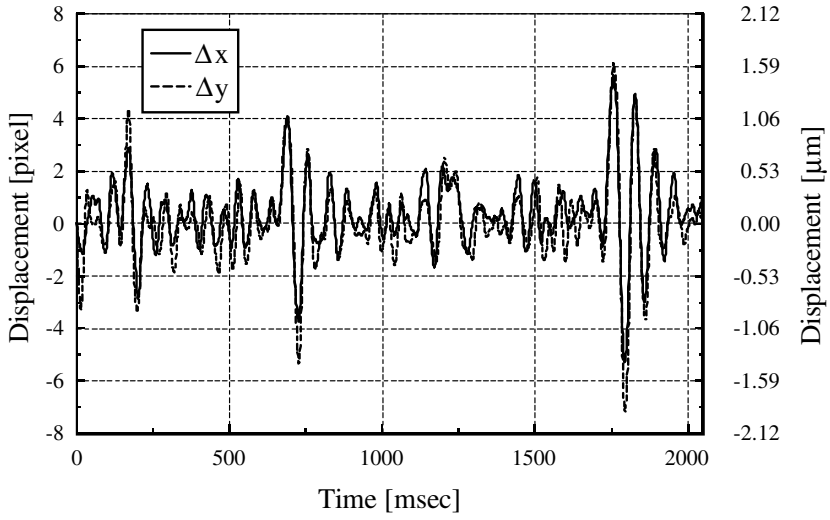

Figure 3. Time series of mesentery motion.

pixels in the x-direction and -1.73 pixels in the y-direction, corresponding to -0.14 and -0.45 μm, respectively. The gradients and variation in displacement in the upper and lower areas of the arteriole were small. It is considered that the motion entirely involved parallel translation, without higher order displacements such as deformation or rotation. This means that the mesentery moved in the direction of lower left. Comparing with the displacements in the upper and lower side of arteriole wall in several cross-sections, the differences in displacements were smaller than 0.1 pixels, or 0.027 μm. These results indicate that the contraction and relaxation of blood vessels in the arteriole were too small to measure.

Figure 3 shows the time series of mesentery motion. The displacement was obtained using displacement in the upper and lower areas of the arteriole. A strong correlation between x displacement and y displacement was confirmed, indicating that the mesentery periodically vibrated from upper right to lower left. The amplitude of vibration varied significantly, and the maximum displacement was about 8.9 pixels, or 2.4 μm. A first derivative of the displacement with respect to time gave the instantaneous velocity of the mesentery. The peak frequency of motion was about 16 Hz, obtained by spectrum analyses. As the cardiac cycle of a rat was about 6–7 Hz obtained by monitoring pressure during the experiment, it is considered that this mesentery vibration was caused by intestinum motion, convulsion and so on.

In all previous studies, the RBC velocity vector is obtained by applying the PIV technique to two successive images without taking mesentery motion into account. The relative position of the RBC velocity vector to vessel wall moves with time. Bias error due to mesentery motion interfered with the analysis of instantaneous RBC velocity. An improved technique is proposed here in order to reduce the effect of mesentery motion. Both the blood image and RBC velocity are modified using the mesentery motion obtained in the previous section as follows:

1. Shift blood images by affine transformation using the integer part of the obtained mesentery displacements, by rounding off, in figure 3 in order to make the relative position of the vector to a vessel constant.
2. Apply the PIV technique to two successive shifted images in order to obtain RBC velocity distributions.

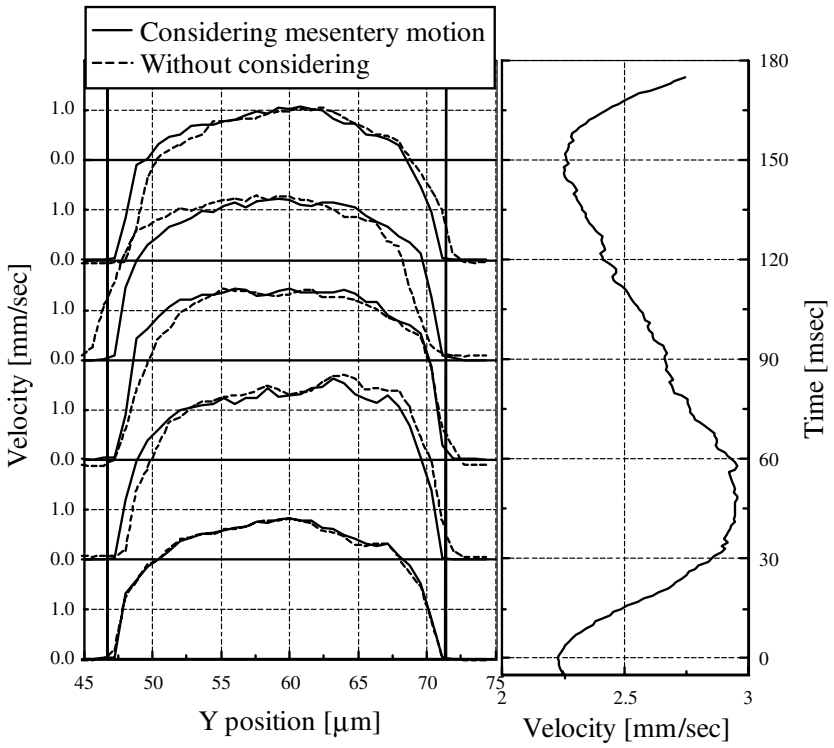

Figure 4. Comparison of instantaneous velocity profiles with and without consideration of mesentery motion during one cardiac cycle for blood flow in arteriole.

3. Subtract the fractional part of the temporal derivations of the mesentery displacements from the obtained velocities in order to improve the bias error.

After the relative positions of the arteriole in all images were arranged consistently and the influence of mesentery motions was removed, the measurement accuracy of RBC velocity was improved. Figure 4 shows a comparison of instantaneous velocity profiles with and without consideration of mesentery motion during one cardiac cycle on blood flow in the arteriole. The profiles on the left are axial blood velocity in cross-section at $x = 85$ μm over approximately 150 ms. The right hand figure shows the time series of RBC velocity averaged across the cross-section. The velocity profiles at $t = 0$ reveal the end of a diastole, and velocities increased sharply towards a peak systole and then decrease gradually towards a late diastole. The velocities obtained by the present method are zero outside the arteriole and maximum around the centre of the arteriole. Conversely, the profiles obtained without consideration of mesentery motion vibrated towards the vessel. This demonstrates the usefulness of this improvement to obtain detailed velocity distributions.

3. Results

Figure 5 shows the instantaneous velocity distributions and time-averaged velocity distributions of 2048 images for 2 s of blood flow in an arteriole, calculated using the PIV technique described in the previous section. The obtained RBC velocity distribution consists of 2047 maps at 1000 Hz. An interrogation window of 7 $\times$ 7 pixels was taken with a 50%

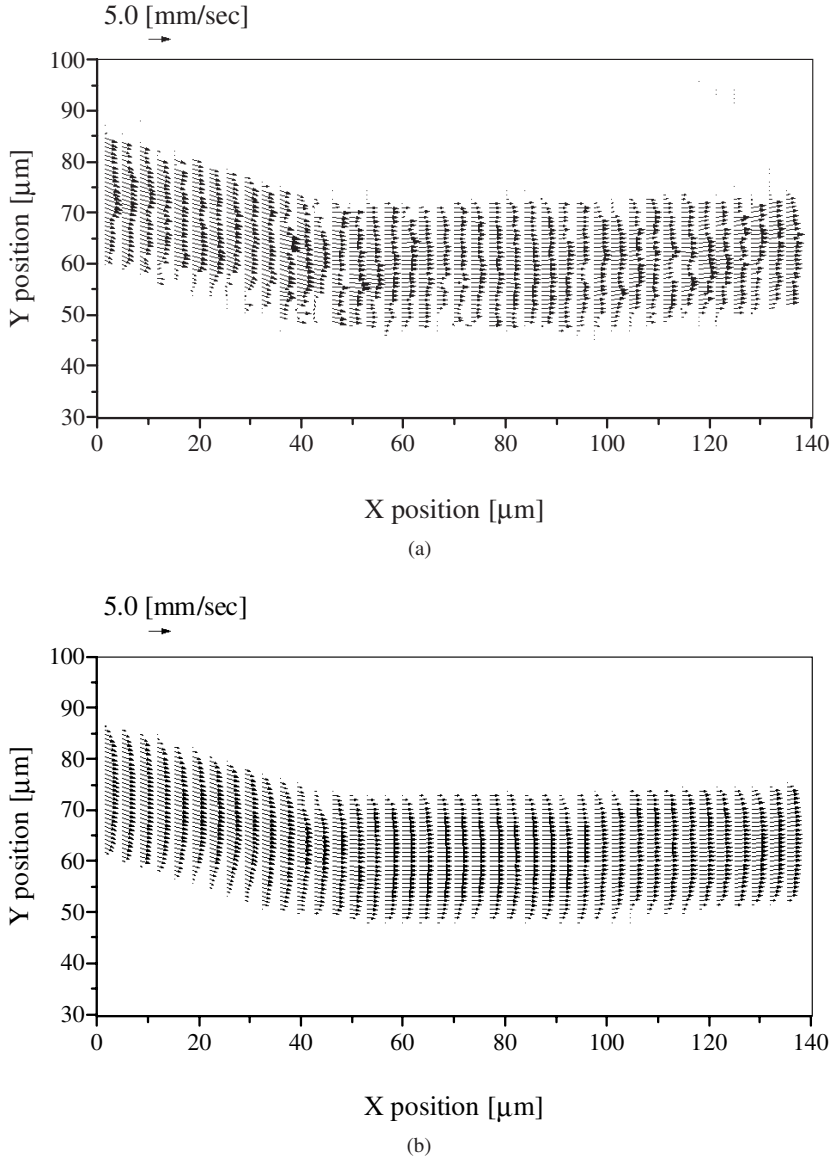

Figure 5. Instantaneous and time-averaged velocity distribution of blood flow in arteriole. (a) Instantaneous velocity distribution. (b) Time-averaged velocity distributions.

overlap, corresponding to a spatial resolution of 0.8×0.8 μm. The velocities in the horizontal direction were thinned out for clarity, by plotting every fourth window. In the results by the improved method, figure 5(a), a velocity distribution with high spatial resolution and high measurement accuracy was obtained. Since the mesentery motion was taken into account, the obtained velocities in the region outside of the arteriole are zero. The maximum instantaneous velocity was about 15.0 pixels/frame or 4.0 mm s^{-1}, which occurred around the centre of the arteriole. The velocity vectors very close to the wall were measured and it was found that the wall-normal components of the velocity vectors were close to zero. Low velocities

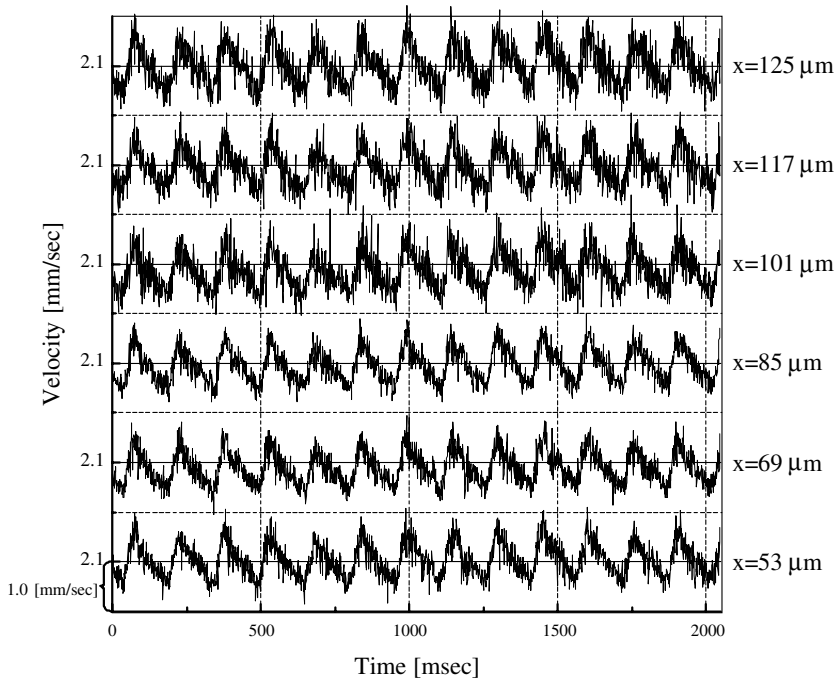

Figure 6. Time series of axial blood velocity averaged in six cross-sections.

were also observed at the inside wall of a blunt corner in the arteriole. This phenomenon was also observed in the time-averaged velocity distribution. It is considered that white blood cells were attached to the vessel wall in that area. Since the interrogation window size was smaller than the size of red blood cells, groups of three to four similar velocity vectors occurred in some regions. Several spurious vectors were observed in the instantaneous velocity distribution. When an RBC did not exit within an interrogation window, a spurious cross-correlation coefficient was obtained for the sub-image. Therefore, statistical values such as time-averaged values were obtained after eliminating such vectors using error correction techniques, in which the vector was determined by comparison with neighbourhood vectors. Spurious vectors were not observed in the averaged velocity in figure 5(b). The maximum velocity was about 11.0 pixels/frame or 3.0 mm s^{-1} at the centre of the arteriole. The velocity vectors on the lower side, at $x = 100$ to 120 μm in particular, were smaller than the values expected for the laminar flow. It is considered that the RBC velocity was reduced due to the presence of a plasma layer.

Figure 6 shows the time series of axial blood velocity averaged in six cross-sections. These values are mean velocities within arteriole profiles at $x = 53$, 69, 85, 101, 117 and 125 μm in figure 1, on the lower stream side at the bend in the vessel. The velocities in every section repeatedly increased sharply towards a peak systole, and then decreased gradually towards a late diastole. The amplitudes and phases in all sections were relatively consistent. The series included 13 cycles. The amplitudes at $t = 650$ to 800 in all the sections became similarly small. High cross-correlations for these series were recognized. The pulsed flow is similar to that of regular circulatory flow. The peak frequency was about 6.4 Hz obtained by spectrum analysis. The result shows that the velocity is synchronized with the cardiac cycle of 6–7 Hz even in microvessels. However, the velocities did not become zero at end diastoles because

of inertia forces. This is consistent with the results obtained in previous studies using the dual-slit method, LDV and other methods. However, some anomalous peaks, such as $x = 69$ μm and $t = 700$, were observed due to the inclusion of spurious vectors. These vectors can be eliminated using error correction techniques. The series at $x = 117$ and 125 μm, on the downstream side, included high-frequency components and exhibited higher amplitudes compared to others.

The axial blood velocity profiles in six sections are shown in figure 7. Thirty velocity values were obtained along the capillary diameter at a spacing of 0.8 μm. The wall positions and capillary diameter in each section are displayed in the figure. The wall position was identified via the luminance of the cross-section in a time-averaged image after mesentery motion compensation. The diameters at $x = 53$, 69, 85, 101, 117 and 125 μm were 24.9, 24.9, 24.7, 25.7, 24.1 and 23.6 μm respectively. The velocity of all profiles became maximal around the centre of the vessel, and decreased to zero near the wall. The arteriole velocity profiles were broad at the centre of the vessel, and sharp near the wall compared with a parabolic flow profile. This suggests that the shear stress on the vessel wall was higher than expected.

The most upstream profile at $x = 53$ μm shown in figure 7(a) is asymmetric. The velocities in the vicinity region of the inner side of the arteriole bend were very low and increased sharply separating from the wall. This is considered to be due to the adherence of leukocytes to the wall on the inner side of the bend, which was conformed using visual observation directly through the microscope. Conversely, the velocities on the outer side increased sharply without a low velocity area. Downstream, the profiles become symmetric, typically at $x = 85$ μm in figure 7(c). The profile at $x = 101$ μm in figure 7(d) in particular shows the typical flow features for a non-Newtonian fluid: a more broad axial velocity distribution and a steep velocity gradient near the wall. The lowest velocity at the centre of vessel and the largest diameter are shown in the profile. A very low velocity region was identified near the right-hand wall due to a marginal cell-free plasma layer. This exhibited the broadest profile. At $x = 117$ μm in figure 7(e), the capillary diameter decreased by about 1.6 μm compared to that upstream, with a corresponding increase in maximum velocity from 3.1 mm s^{-1} to 3.5 mm s^{-1}. A dip in velocity in the central part of the tube was observed. At $x = 125$ μm in figure 7(f), for the smallest diameter section, the dip was not observed and the cell-free plasma layer was less predominant.

4. Discussion

4.1. Measurement accuracy

The optical resolution of the proposed system, based on the wavelength of light ($\lambda = 546$ nm) and the numerical aperture of the lens (NA = 1.0) is 0.33 μm. The vertical and horizontal resolution of 0.27 μm was finer than the optical resolution. However, the luminance distribution of red blood cells was preserved spatially and temporally. The smallest measurable displacement by the present method is approximately 1% of the image resolution, or about 3 μm s^{-1}. This is achieved through gradient-based sub-pixel analysis with luminance information and a 256 greyscale (Sugii *et al* 2000). Since the precision of the technique was affected by the displacement gradient, out-of-plane motion, image noise and so on, these effects are assessed below.

According to the result for mesentery motion in section 2.2, the displacement varied from -1.9 to 1.6 μm in the y-direction from the reference position, and the instantaneous velocity of the mesentery also varied from -0.26 to 0.17 mm s^{-1} in the x-direction. These amplitudes correspond to about 14% of the vessel diameter and 13% of the time-averaged RBC velocity

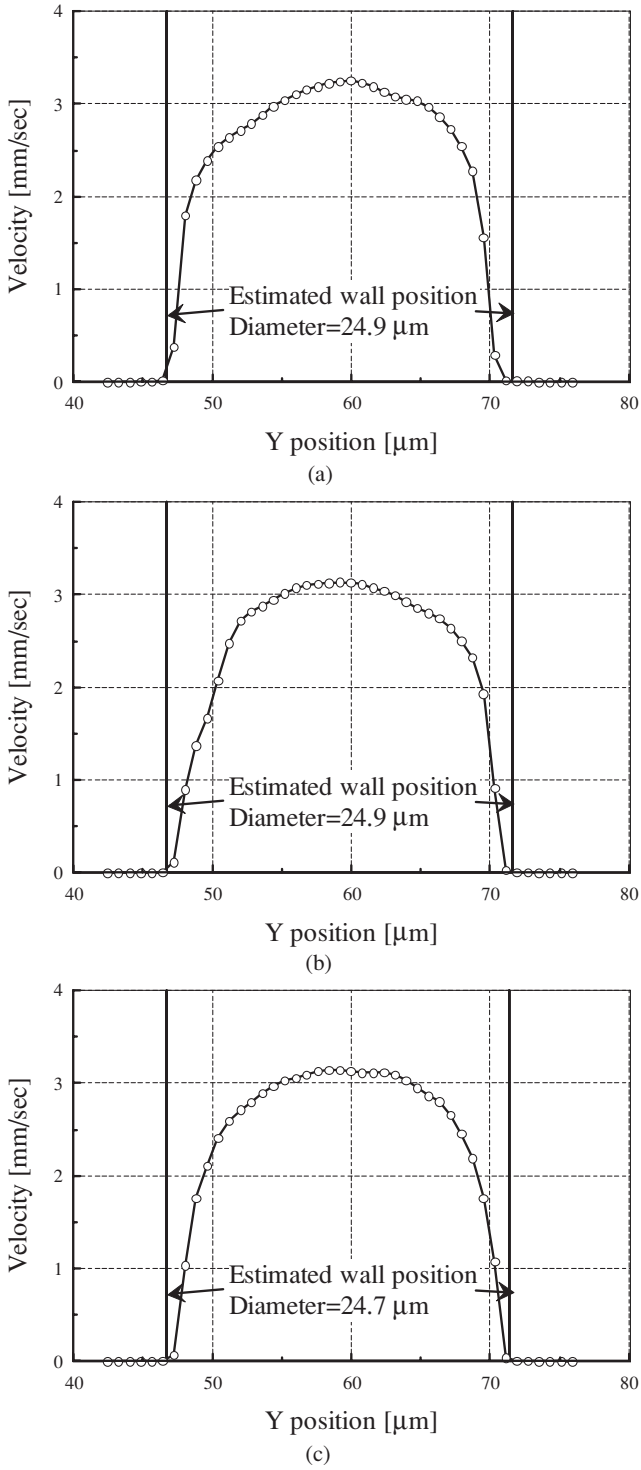

Figure 7. Cross-sectional time-averaged axial velocity profiles for six cross-sections. (a) $x = 53$ μm, (b) $x = 69$ μm, (c) $x = 85$ μm, (d) $x = 101$ μm, (e) $x = 117$ μm and $x = 125$ μm.

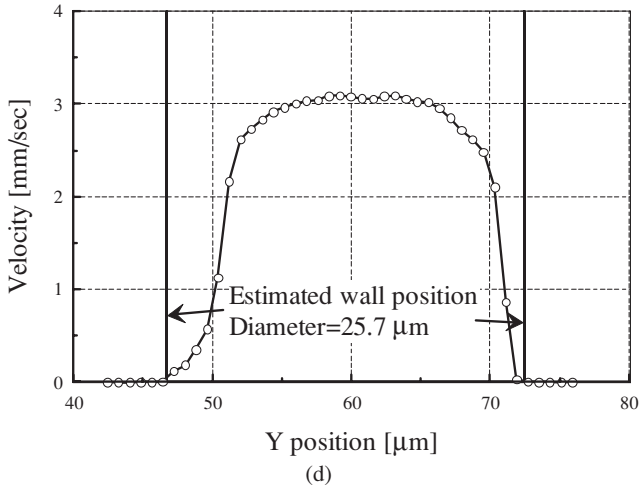

(d)

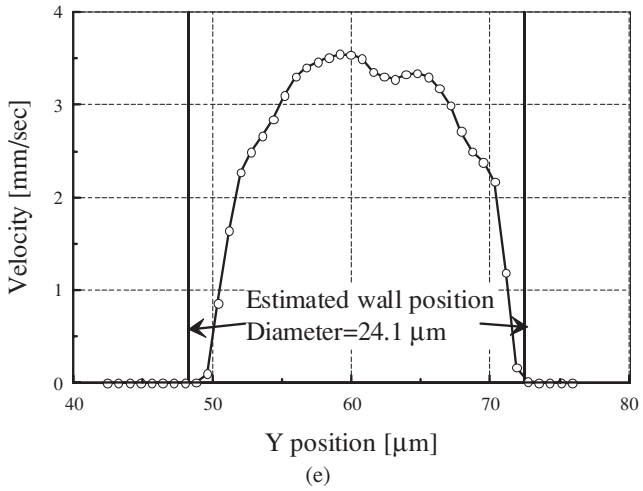

(e)

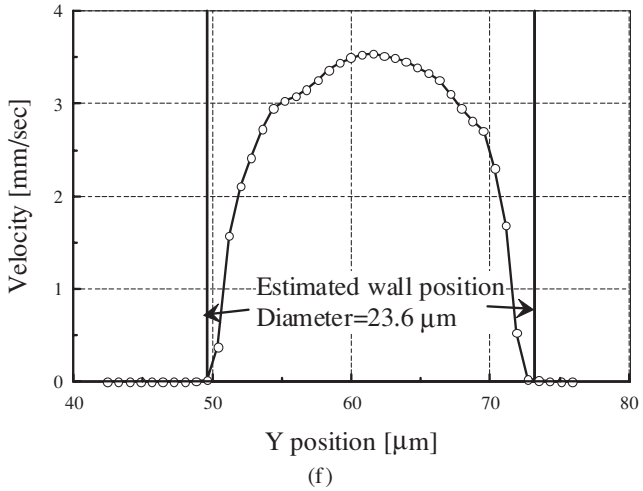

(f)

Figure 7. (Continued.)

at the centre of the vessel, respectively. Without taking the motion into account, the time-averaged and spatially averaged velocity exhibited a broad profile, and bias error of 13% was introduced. In large vessels, the effect was reduced by attaching the sensor on the outer wall of the vessel in the dual-slit method. However, it is difficult to improve the measurement error for microcirculation.

The obtained velocity vector represents integrated values of velocities in the volume, which is determined by the size of interrogation window and the depth of focus. It was reported that the depth of focus of a microscope objective lens was a function of the refractive index of the fluid between the subject flow and the objective, the wavelength of light, the numerical aperture of the objective and so on (Born and Wolf 1997, Meinhart *et al* 2000). In these experiments, the depth of focus was as shallow as approximately 2 μm using a water-immersion objective with a high numerical aperture. The velocity gradient often reduces measurement accuracy because the obtained vector is a weighted average within the volume (Olsen and Adrian 2000) and it is assumed that the velocity is constant within an interrogation window. Since red blood cells are larger than the measurement volume, the velocity gradient within a cell is small. Therefore, the displacement of a cell can be obtained correctly. However, since the gradient between the approaching RBCs may become large, the accuracy near the boundary of a cell is reduced. As cells are excited randomly in space and time, the statistical value of RBC velocity is considered to be reasonable.

In the measurement of two-dimensional velocity, the correlation coefficient is spoiled due to the appearance and disappearance of particles in the plane. Therefore, any out-of-plane motion reduces the measurement accuracy. In the experiments, the out-of-velocity component, defined by the displacement in the depth direction with respect to the depth of focus, was negligible in comparison to the size of the cell. The effect of the appearance and disappearance of particles can therefore be ignored.

4.2. Comparison of time-averaged velocity profiles in different cross-sections

Although the temporal resolution of the present method was coarser than that of the dual-slit method, spatial resolution is significantly improved. It was difficult to obtain the velocity profile and estimate the wall shear rate from the results of the dual-slit method. Differences between the time-averaged velocity profiles for different geometries of arteriole segments, such as vessel diameter, were recognized in figure 7. An increase in the velocity profile downstream of the bend in the arteriole was observed due to constriction acceleration induced by the adherence of leukocytes to the inner wall of the bend, which was confirmed by visual observation. The profile revealed the typical flow features of non-Newtonian fluids: a broader axial velocity and a steep velocity gradient near the wall at the largest diameter section. There is good agreement with a previous study in that the profile becomes broader with decreasing maximum velocity in a section or capillary diameter (Bishop *et al* 2001). However, differences in velocity profiles due to varying capillary diameter as a result of wall aberrations have never been reported. This suggests that the velocity profile and wall shear stress are sensitive to the geometry of the vessel. The very low velocity region near the wall due to a marginal cell-free plasma layer was also observed, attributable to multi-phase flow.

5. Conclusion

The PIV method was applied to determine mesentery motion, and improved the accuracy of RBC velocity by taking the motion into account. Images were recorded using an intravital microscope with water-immersion objective lens and metal-halide back-illumination, and

high-speed digital video system. Rat mesentery motion and RBC velocity distributions of the arteriole were obtained with high temporal and spatial resolution. Velocity distributions with spatial resolutions of 0.8×0.8 μm were measured even near the wall in the centre plane of the arteriole. The measurement accuracy was improved by taking mesentery motion into account. Pulsed flow caused by the cardiac cycle was observed. The velocity profile was broad at the centre of the vessel and sharp near the wall. Differences in the axial velocity profiles in six cross-sections were also observed, attributed to variations in the diameter of the vessel and the extent of the plasma layer. Furthermore, the flow features for non-Newtonian fluid were observed. The results indicate that the proposed method is very useful for the measurement of blood flow velocity profiles with high temporal and spatial resolution.

Acknowledgments

The authors would like to express their appreciation to Dr Niimi of the National Cardiovascular Center of Japan for valuable discussion, and Mr Nakano and Dr Minamiyama of the National Cardiovascular Center for offering high-speed video image.

References

Bishop J J, Nance P R, Popel A S, Intaglietta M and Johnson P C 2001 Effect of erythrocyte aggregation on velocity profiles in venules *Am. J. Physiol. Heart Circ. Physiol.* **280** H222–H236

Born M and Wolf E 1997 *Principles of Optics* (Oxford: Pergamon)

Cochrane T, Earnshaw J C and Love A H G 1981 Laser Doppler measurement of blood velocity in microvessels *Med. Biod. Eng. Comput.* **19-15** 589–96

Intaglietta M, Silverman N R and Tompkins W R 1975 Capillary flow velocity measurements in vivo and in situ by television methods *Microvasc. Res.* **10** 165–79

Keane R D and Adrian R J 1992 Theory of cross-correlation analysis of PIV images *Appl. Sci. Res.* **49** 191–215

Koutsiaris A G, Mathioulakis D S and Tsangaris S 1999 Microscope PIV for velocity-field measurement of particle suspensions flowing inside glass capillaries *Meas. Sci. Technol.* **10** 1037–46

Meinhart C D, Wereley S T and Santiago J G 1999 PIV measurement of a microchannel flow *Exp. Fluids* **27** 414–9

Meinhart C D, Wereley S T and Gray M H B 2000 Volume illumination for two-dimensional particle image velocimetry *Meas. Sci. Technol.* **11** 809–14

Nakano A, Minamiyama M, Sugii Y and Nishio S 2001 Measurement of red blood cell velocity profile in microvessels using particle image velocimetry combined with high-speed digital camera *Microcirc. Annu.* **17** 159–60

Nakano A, Sugii Y, Minamiyama M and Niimi H 2002 Measurements of red cell velocity profiles in rat mesentery arterioles using particle image velocimetry and high-speed videomicroscopy *Micr. Vasc. Res.* submitted

Olsen M G and Adrian R J 2000 Out-of-focus effects on particle image visibility and correlation in microscopic particle image velocimetry *Exp. Fluids Suppl.* S166–S174

Parthasarahi A A, Japee S A and Pittman R N 1999 Determination of red blood cell velocity by shuttering and image analysis *Ann. Biomed. Eng.* **27** 313–25

Raffel M, Willert C E and Kompenhans J 1998 *Particle Image Velocimetry* (Berlin: Springer)

Santiago J G, Wereley S T, Meinhart C D, Beebe D J and Adrian R J 1998 A particle image velocimetry system for microfluidics *Exp. Fluids* **25** 316–9

Seki J, Sasaki Y, Oyama T and Yamamoto J 1996 Fiber-optic laser-Doppler anemometer microscope applied to the cerebral microcirculation in rats *Biorheology* **33** 463–70

Sugii Y, Nakano A, Nishio S and Minamiyama M 2001 Blood flow velocity measurement in microcirculation field by means of highly accurate iterative PIV *Trans. Japan Society of Mechanical Engineers* **67-662** 2431–6 (in Japanese)

Sugii Y, Nishio S, Okuno T and Okamoto K 2000 A highly accurate iterative PIV technique using gradient method *Meas. Sci. Technol.* **11** 1666–73

Tangelder G J, Slaaf D W, Arts T and Reneman R S 1988 Wall shear rate in arterioles in vivo: least estimates from platelet velocity profiles *Am. J. Physiol.* **254** H1059–H1064

Tangelder G J, Slaaf D W, Muijtjens A M M, Arts T, oude Egbrink M G A and Reneman R S 1986 Velocity profiles of blood platelets and red blood cells flowing in arterioles of the rabbit mesentery *Circ. Res.* **59** 505–14

Tsukada K, Minamitani H, Sekizuka E and Oshio C 2000 Image correlation method for measuring blood flow velocity in microcirculation: correlation 'window' simulation and *in vivo* image analysis *Physiol. Meas.* **21** 459–71

Yamaguchi S, Yamakawa T and Niimi H 1992 Red cell velocity and microvessel diameter measurement by a two fluorescent tracer method under epifluorescence microscopy: application to cerebral microvessels of cats *Int. J. Microcirc.* **11** 403–16

Wayland H and Johnson P C 1967 Erythrocyte velocity measurement in microvessels by two-slit photometric method *J. Appl. Physiol.* **22** 333–7